

SCIENTIFIC REPORTS

OPEN

Element-Specific Orbital Character in a Nearly-Free-Electron Superconductor $\text{Ag}_5\text{Pb}_2\text{O}_6$ Revealed by Core-Level Photoemission

Soobin Sinn^{1,2}, Kyung Dong Lee³, Choong Jae Won³, Ji Seop Oh^{1,2}, Moon-sup Han⁴, Young Jun Chang⁴, Namjung Hur³, Byeong-Gyu Park⁵, Changyoung Kim^{1,2}, Hyeong-Do Kim^{1,2,6} & Tae Won Noh^{1,2}

$\text{Ag}_5\text{Pb}_2\text{O}_6$ has attracted attentions due to its novel nearly-free-electron superconductivity, but its electronic structure and orbital character of the Cooper-pair electrons remain controversial. Here, we present a method utilizing core-level photoemission to show that Pb 6s electrons dominate near the Fermi level. We observe a strongly asymmetric Pb 4 $f_{7/2}$ core-level spectrum, while a Ag 3 $d_{5/2}$ spectrum is well explained by two symmetric peaks. The asymmetry in the Pb 4 $f_{7/2}$ spectrum originates from the local attractive interaction between conducting Pb 6s electrons and a Pb 4 $f_{7/2}$ core hole, which implies a dominant Pb 6s contribution to the metallic conduction. In addition, the observed Pb 4 $f_{7/2}$ spectrum is not explained by the well-known Doniach-Šunjić lineshape for a simple metal. The spectrum is successfully generated by employing a Pb 6s partial density of states from local density approximation calculations, thus confirming the Pb 6s dominant character and free-electron-like density of states of $\text{Ag}_5\text{Pb}_2\text{O}_6$.

Since the discovery of the high-temperature superconducting cuprate¹, two-dimensional layered oxide superconductors have become a central research subject in condensed matter physics². $\text{Ag}_5\text{Pb}_2\text{O}_6$ was recently added to the list. Figure 1 shows its layered crystal structure, in which the PbO_3 honeycomb layer is sandwiched between two types of Ag layers. Despite its low T_c of 52.4 mK³, the material has attracted attentions because of its nearly-free-electron nature in the normal metallic phase^{4,5}. Typical nearly-free-electron materials, such as alkali and noble metals, do not exhibit superconductivity at ambient pressure, except Li, which has an extremely low T_c of 0.4 mK⁶. Therefore, $\text{Ag}_5\text{Pb}_2\text{O}_6$ has been considered an ideal model system for investigating superconductivity without the effects of the complicated electronic structure.

For superconductors, understanding which electrons will participate in Cooper pairing is important. However, the conduction-state formation of $\text{Ag}_5\text{Pb}_2\text{O}_6$ remains controversial. Assuming the formal valencies of Ag, Pb, and O ions of +1, +4, and −2, respectively, the material should have one excess electron per chemical formula, which will contribute to free-electron-like conduction. A simple look at the crystal structure suggests that the excess electron may belong to the Ag layers. An earlier extended Hückel tight-binding study also suggested that only the Ag 5s orbital contributes to the conduction of the material⁷. In contrast, a recent theoretical study using local density approximation (LDA) suggested a different electronic structure, wherein a Pb 6s orbital hybridized with O 2p orbitals crosses the Fermi level (E_F), forming a nearly-free-electron band⁴.

Several experimental studies have attempted to understand the valence state of this material. Some bond length analyses were performed but provided contradicting results regarding the distinction between Ag-dominant^{8,9} and Pb-dominant¹⁰ characters, while de Haas-van Alphen measurements⁵ demonstrated a nearly-free-electron

¹Center for Correlated Electron Systems, Institute for Basic Science (IBS), Seoul, 08826, Republic of Korea.

²Department of Physics and Astronomy, Seoul National University (SNU), Seoul, 08826, Republic of Korea.

³Department of Physics, Inha University, Incheon, 22212, Republic of Korea. ⁴Department of Physics, University of Seoul, Seoul, 02504, Republic of Korea. ⁵Pohang Accelerator Laboratory, Pohang University of Science and Technology, Pohang, 37673, Republic of Korea. ⁶Present address: Pohang Accelerator Laboratory, Pohang University of Science and Technology, Pohang, 37673, Republic of Korea. Correspondence and requests for materials should be addressed to H.-D.K. (email: hdkim6612@postech.ac.kr) or T.W.N. (email: twnoh@snu.ac.kr)

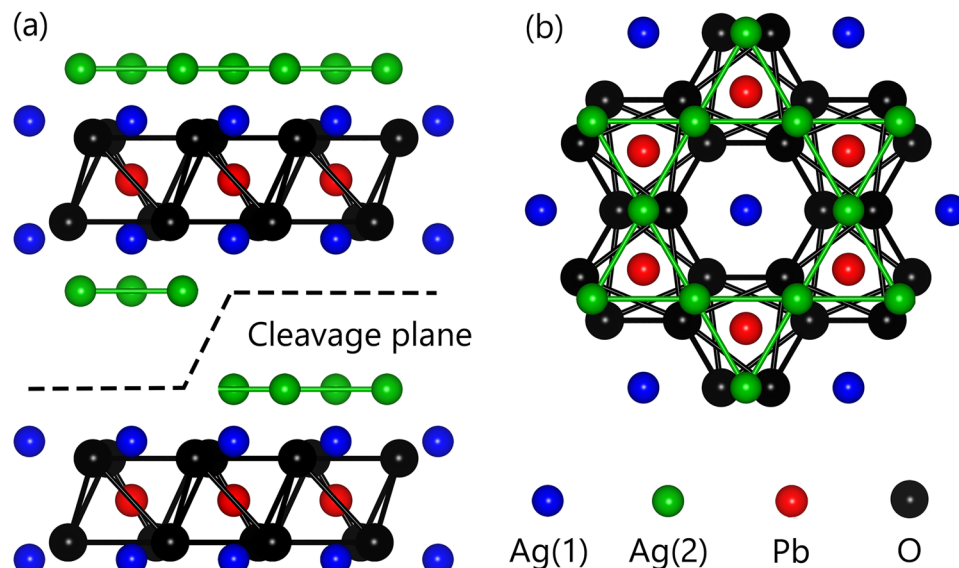


Figure 1. (a) Side view and (b) top view of the crystal structure of $\text{Ag}_5\text{Pb}_2\text{O}_6$. Green, blue, red, and black spheres represent Ag(1), Ag(2), Pb, and O ions, respectively. Two possible cleavage planes with Ag(1) and Ag(2) terminations are shown as a dashed line.

Fermi surface and indirectly supported the validity of the LDA scenario⁴. The only direct experimental evidence was from X-ray absorption spectroscopy (XAS), which suggested that the conduction electrons may be formed by the Pb 6s orbital¹⁰. However, the absorption edge in the XAS was not sharp enough to provide decisive experimental evidence.

Valence-band photoemission measurements have served as an ideal tool for identifying the orbital character because they can directly probe valence bands of a solid. Each orbital has a distinct photon-energy dependence in photoionization cross sections¹¹. By varying the incident photon energies, photoemission spectra can be tuned to obtain the orbital-selective partial density of states (DOS) of valence bands¹². However, in case of $\text{Ag}_5\text{Pb}_2\text{O}_6$, the photon-energy dependence of photoionization cross sections of Ag 5s and Pb 6s orbitals are quite similar¹¹. Therefore, investigating the orbital characters of $\text{Ag}_5\text{Pb}_2\text{O}_6$ using valence-band photoemission is difficult.

Here, we present an alternative approach that utilizes core-level photoemission to investigate the element-specific orbital characters of the conduction electrons in $\text{Ag}_5\text{Pb}_2\text{O}_6$. We show that the detailed core-level lineshape, especially its asymmetry, is strongly influenced by the Coulomb interaction between a core hole and conduction electrons. We observe strong asymmetry in a Pb 4 $f_{7/2}$ core-level spectrum, while a Ag 3 $d_{5/2}$ spectrum is nearly symmetric. This difference implies that the Pb 6s conduction electrons are dominant near E_F . We also demonstrate that the asymmetry of the core-level spectrum can be understood quantitatively based on the Mahan-Nozières-DeDominicis (MND) theory^{13–15}. The Pb 4 $f_{7/2}$ spectrum of $\text{Ag}_5\text{Pb}_2\text{O}_6$ cannot be explained by the Doniach-Šunjić (DŠ) lineshape¹⁶, which has been widely used to explain the core-level spectra of many metallic materials. By entering a realistic DOS of the Pb 6s orbital⁴ into the MND model, we can successfully explain the lineshape quantitatively. Our fit results support the LDA results; i.e., $\text{Ag}_5\text{Pb}_2\text{O}_6$ has a free-electron-like electronic structure but with a narrow bandwidth.

Results and Discussion

The Ag 3 $d_{5/2}$ and Pb 4 $f_{7/2}$ core-level spectra of $\text{Ag}_5\text{Pb}_2\text{O}_6$ are shown in Fig. 2(a) and (b), respectively. Both spectra are fitted by symmetric Lorentzian peaks convoluted by a Gaussian after subtracting Shirley backgrounds¹⁷. Red lines in Fig. 2 represent the results of the fitting. To verify any surface contributions, we measured core-level spectra at takeoff angles of 0° and 60°. At 60°, the effective probing depth should be half that of 0°. Thus, in the spectrum with a 60° takeoff angle, a surface peak should be much more intense than the bulk peaks. However, as shown in the insets of Fig. 2, the spectral differences between the 0° and 60° spectra are negligible, which confirms the absence of surface-state contributions.

As shown in Fig. 2(a), Ag 3 $d_{5/2}$ core-level spectrum can be well described by two symmetric peaks with a Lorentzian full-width at half-maximum (FWHM) of 0.274 eV¹⁸, which we attribute to two crystallographic Ag sites: Ag(1) and Ag(2) as schematically displayed in Fig. 1. The intensity ratio between these two peaks can be determined using the emission depth distribution function¹⁹. To evaluate the function, we calculated the inelastic mean free path using the TPP-2M equation²⁰ embedded in the NIST Electron Inelastic-Mean-Free-Path Database (<https://www.nist.gov/srd/nist-standard-reference-database-71>). Using the value of 4.93 Å for the inelastic mean free path, we evaluated the emission depth distribution function. With a calculated ratio of Ag(1): Ag(2) = 1: 1.58, we could obtain a good fit as shown in Fig. 3(a). The small discrepancy between the experimental and fit results may be due to the imperfection of the sample surface. Conversely, the Pb 4 $f_{7/2}$ core-level spectrum cannot

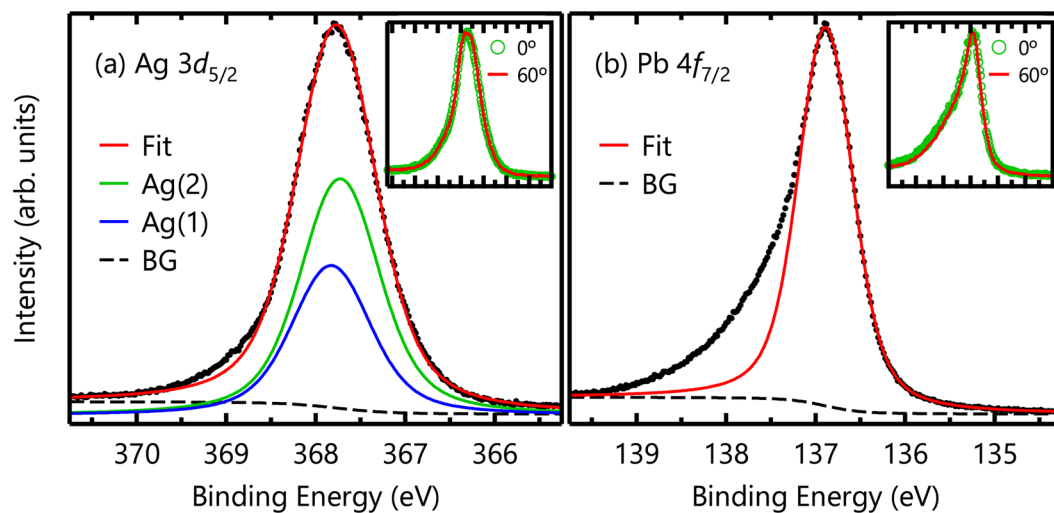


Figure 2. (a) Ag $3d_{5/2}$ and (b) Pb $4f_{7/2}$ core-level spectra of $\text{Ag}_5\text{Pb}_2\text{O}_6$. Red lines represent results fitted by symmetric Lorentzian peaks. The insets show the takeoff-angle dependence in each spectrum. The negligible differences imply that there are no surface states in either spectra.

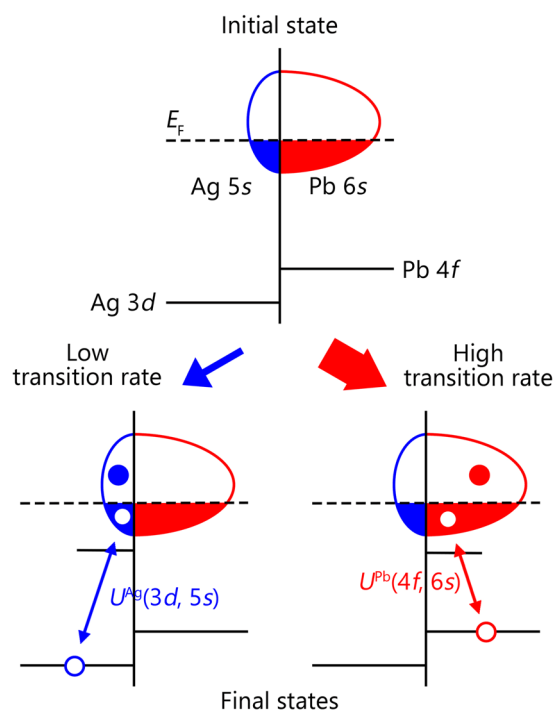


Figure 3. Schematic diagram of core-level photoemission in $\text{Ag}_5\text{Pb}_2\text{O}_6$. A Pb-dominant character is assumed for the conduction electrons in the diagram. A Coulomb interaction between a Pb core hole and Pb conduction electrons generates electron-hole pairs in the E_F -crossing band.

be explained by a single symmetric peak, leaving a large amount of spectral weight at high binding energies as shown in Fig. 2(b).

The strong asymmetry of the Pb $4f_{7/2}$ spectrum should be directly related to dominant Pb 6s partial DOS near the E_F . Figure 3 schematically shows the core-level photoemission processes in $\text{Ag}_5\text{Pb}_2\text{O}_6$. Local Coulomb interaction by a core photohole will scatter conduction electrons, thus exciting electron-hole pairs in a E_F -crossing band. Due to the local attractive core-hole potential, an impurity-like state appears below the bottom of the valence band. The energies of the final states with electron-hole pair excitations are higher than that of the lowest energy state, resulting in a large spectral weight at a high binding energy and an asymmetric core-level lineshape. In $\text{Ag}_5\text{Pb}_2\text{O}_6$, we observed that a Ag $3d_{5/2}$ spectrum is nearly symmetric, indicating few excitations at the Ag 5s conduction band. In contrast, the Pb $4f_{7/2}$ core-level spectrum is highly asymmetric, which implies that many

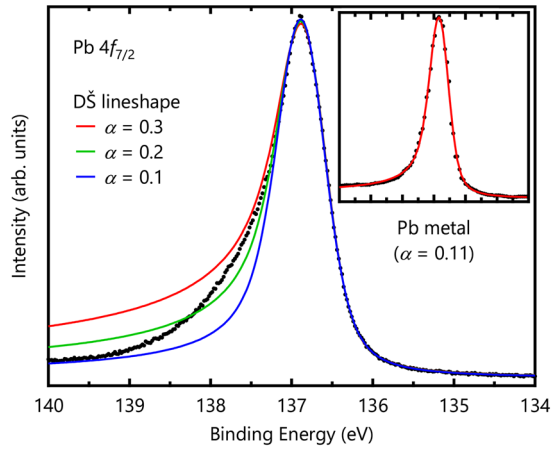


Figure 4. Pb $4f_{7/2}$ core-level spectrum and fitting results of the DŠ lineshape with several values. The inset shows a Pb $4f_{7/2}$ core-level spectrum of a Pb metal from ref. 24, which is well explained by the DŠ lineshape with $\alpha = 0.11$.

electron-hole pairs are excited at the Pb $6s$ conduction band as shown in Fig. 3. Therefore, the main character of the conduction electrons in $\text{Ag}_5\text{Pb}_2\text{O}_6$ should be the Pb $6s$ electrons.

The asymmetric core-level lineshape in a metal can be understood based on the MND theory^{13–15}, in which a local Coulomb potential due to a core hole scatters conduction electrons. The model Hamiltonian is given by

$$H = \sum_{\mathbf{k}} \varepsilon_{\mathbf{k}} c_{\mathbf{k}}^{\dagger} c_{\mathbf{k}} + \varepsilon_h h^{\dagger} h - \frac{U}{N} \sum_{\mathbf{k}\mathbf{k}'} c_{\mathbf{k}}^{\dagger} c_{\mathbf{k}'} h^{\dagger} h, \quad (1)$$

where $c_{\mathbf{k}}^{\dagger}$ ($c_{\mathbf{k}}$) is an conduction-electron creation (annihilation) operator, h^{\dagger} (h) a core-hole creation (annihilation) operator, $\varepsilon_{\mathbf{k}}$ a conduction-electron energy with a momentum \mathbf{k} , ε_h a core-hole energy, and N the number of lattice sites considered in the model. U is an attractive on-site Coulomb interaction between conduction electrons and a core hole. Without U , the core-level spectrum should have a simple Lorentzian lineshape, whose half width at half-maximum γ reflects a core-hole lifetime. By turning on U , electron-hole pairs can be excited across the E_F , resulting in an asymmetric lineshape. Thus, a quantitative analysis of an asymmetric spectral function $A(\omega)$ can provide us with important information regarding conduction bands, such as U and DOS near the E_F .

In the MND theory, if a conduction-band has a flat DOS with an infinite energy range, $A(\omega)$ can be expressed in a closed form, which yields the well-known DŠ lineshape¹⁶:

$$A_{D\check{S}}(\omega) = \frac{\Gamma(1 - \alpha) \cos[\pi\alpha/2 + (1 - \alpha)\tan^{-1}(\omega/\gamma)]}{(\omega^2 + \gamma^2)^{(1-\alpha)/2}}, \quad (2)$$

where $\Gamma(x)$ is the gamma function and α is an asymmetry parameter. This simple spectral function greatly reduces a numerical cost compared to the general MND model. When $\alpha = 0$, the lineshape is just a symmetric Lorentzian of half-width γ . According to the MND theory, α is approximately given by $U^2 \rho^2(E_F)$ at the weak-coupling limit, where $\rho(\varepsilon)$ is the conduction-band DOS¹⁶. Because of the strong locality of U , the strength of asymmetry α should be related to an element-specific partial DOS. Note that the DŠ lineshape has been quite successful at describing core-level spectra from numerous metals, such as noble²¹ and simple^{22,23} metals.

However, the measured Pb $4f_{7/2}$ spectrum is not explained by the simple DŠ lineshape. Figure 4 shows several trial fits of the Pb $4f_{7/2}$ core-level spectrum wherein the value of α using Eq. (2) is varied. When α is small, the large asymmetry cannot be explained. Conversely, large α values render large tails at higher binding energies. The inset of Fig. 4 shows a Pb $4f_{7/2}$ core-level spectrum of the Pb metal from ref. 24, which is well explained by the DŠ lineshape with $\alpha = 0.11$, unlike the case of $\text{Ag}_5\text{Pb}_2\text{O}_6$. This discrepancy may be ascribed to the assumption of the flat, broad conduction-band DOS used to obtain the DŠ lineshape. A similar discrepancy in the DŠ lineshape behavior has also been reported in narrow d -band metals such as Pd and Pt²¹.

To explain the asymmetric lineshape at a quantitative level, we adopted a theoretical approach reported by Davis and Feldkamp^{25,26}. The model reads

$$H = \int \varepsilon \psi_{\varepsilon}^{\dagger} \psi_{\varepsilon} d\varepsilon + \varepsilon_h h^{\dagger} h - \iint \tilde{U}(\varepsilon, \varepsilon') \psi_{\varepsilon}^{\dagger} \psi_{\varepsilon'} h^{\dagger} h d\varepsilon d\varepsilon', \quad (3)$$

where $\psi_{\varepsilon}^{\dagger}$ (ψ_{ε}) is a creation (annihilation) operator of a conduction electron with an energy ε . Here, \tilde{U} is given by

$$|\tilde{U}(\varepsilon, \varepsilon')|^2 = U^2 \rho(\varepsilon) \rho(\varepsilon'). \quad (4)$$

After the creation of a core hole, a final one-electron eigenstate ϕ_n with an energy eigenvalue ω_n is given by a unitary transformation $S_n(\varepsilon)$ of the initial eigenstate ψ_{ε} : i.e.

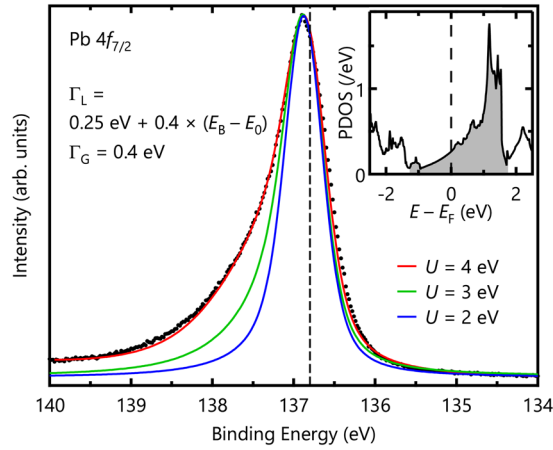


Figure 5. Pb $4f_{7/2}$ core-level spectrum and fitting results of MND-model calculations with the Pb $6s$ partial DOS. The spectrum is well explained with $U = 4$ eV. The dashed line represents the lowest binding energy of 136.8 eV. The inset shows the Pb $6s$ partial DOS from LDA calculations, and the gray shaded region was considered in our calculations.

$$\varphi_n = \int S_n(\varepsilon) \psi_\varepsilon d\varepsilon. \quad (5)$$

After discretizing the energy for numerical calculations, a final many-body state Φ_α is given by a product of L eigenstates: $\Phi_\alpha = \varphi_{n_1} \varphi_{n_2} \cdots \varphi_{n_L}$, with an energy of $E_\alpha = \omega_{n_1} + \omega_{n_2} + \cdots + \omega_{n_L}$, while its spectral intensity is given by $|\langle \Phi_\alpha | \Phi_G \rangle|^2$, where Φ_G corresponds to the initial many-body ground state with the lowest occupied L eigenstates. Note that $|\langle \Phi_\alpha | \Phi_G \rangle|^2$ corresponds to the square of a determinant of an order- L matrix whose elements are $S_n(\varepsilon)$. When $\rho(\varepsilon)$ is given, we can easily calculate $S_n(\varepsilon)$ and its associated spectral intensity. Then, the spectral function $A(\omega)$ is given by the total sum of spectral contributions of the ${}_N C_L$ final states.

To explain our Pb $4f_{7/2}$ spectrum, we calculated the spectral function by employing the realistic Pb $6s$ partial DOS from LDA calculations⁴. An experimental DOS from valence-band photoemission would not be useful, because it is difficult to extract the contribution from Ag and Pb from the partial DOS of E_F -crossing bands by varying the incident phonon energy as mentioned earlier. Moreover, the photoemission spectrum does not provide information above E_F . Instead, we employed the Pb $6s$ partial DOS from LDA calculations as shown in the inset of Fig. 5. According to the MND theory, completely filled or empty conduction bands are not responsible for the asymmetric lineshape, because there is a finite energy gap for electron-hole pair excitations, and their spectral contributions are negligible compared with those from excitations in E_F -crossing bands. To calculate a Pb $4f_{7/2}$ core-level spectrum, we used the partial DOS from -1.27 to 1.72 eV (the gray shaded region in the inset of Fig. 5), which corresponds to the minimum or maximum of the E_F -crossing band, respectively⁴. In our calculations, final states with one or two electron-hole pair creations are considered to have a total spectral weight larger than 0.999.

The observed Pb $4f_{7/2}$ spectrum is quantitatively well explained by the MND calculations as shown in Fig. 5. To compare it with the experimental spectrum, we convoluted them using a Lorentzian and a Gaussian functions. For the Lorentzian broadening, we used $\Gamma_L = 0.25$ eV $+ 0.4 \times (E_B - E_0)$ (FWHM), where the first (second) term corresponds to a lifetime for the core hole (electron-hole pair). E_0 is the lowest binding energy in the calculations. The E_0 value was set to 136.8 eV for the Pb $4f_{7/2}$ spectrum as represented by the dashed line in Fig. 5. To account for the extrinsic broadening, we also included a Gaussian broadening with $\Gamma_G = 0.4$ eV (FWHM) in the calculations. The calculated spectrum with $U = 4$ eV reproduced the observed Pb $4f_{7/2}$ spectrum quite well. The lineshape of the high-binding-energy tail is strongly governed by the shape of DOS²⁷. Therefore, the success of our MND calculations supports the validity of the LDA calculations⁴, which suggested the Pb $6s$ character of charge carriers and the free-electron-like electronic structure.

For comparison, we also depict calculation results with $U = 2$ and 3 eV in Fig. 5. The figure clearly shows that the asymmetries of the calculated spectra are quite sensitive to the values of U . Since the asymmetry parameter is approximately given by $U^2 \rho^2(E_F)$ in the DS lineshape¹⁶, asymmetry in a core-level spectrum is a good indicator of an element-specific contribution to metallic behavior at similar values of U . According to Hartree-Fock calculations for atomic orbitals using Cowan's code²⁸, the average values of bare Coulomb interaction U_0 between a core hole and conduction electrons for Ag $3d$ - $5s$ and Pb $4f$ - $6s$ electrons are

$$U_0^{\text{Ag}}(3d, 5s) = F_{\text{Ag}}^0(3d, 5s) - 1/10 G_{\text{Ag}}^2(3d, 5s) = 11.7 \text{ eV}, \quad (6)$$

and

$$U_0^{\text{Pb}}(4f, 6s) = F_{\text{Pb}}^0(4f, 6s) - 1/14 G_{\text{Pb}}^3(4f, 6s) = 14.9 \text{ eV}, \quad (7)$$

respectively, where F^0 , G^2 , and G^3 are Slater integrals²⁹. These values of the bare interactions are considerably reduced due to the screening by conduction electrons. Using the relation between the screened Coulomb

interaction U and a polarization P , $U = U_0/(1 - PU_0)^{30}$, we can estimate the value of $U^{Ag}(3d, 5s)$ to be 3.7 eV from $U^{Pb}(4f, 6s) = 4$ eV, assuming the same polarization for each core hole. Those values are so similar that we can expect a highly asymmetric lineshape for the Ag 3 $d_{5/2}$ spectrum, in contrast to the real one. Thus, we can conclude that the Ag 5s partial DOS at E_F should be much smaller than that of Pb 6s.

Conclusion

We settled the controversy surrounding the element-specific orbital character of $Ag_5Pb_2O_6$ by measuring its core-level photoemission spectra. The dominant Pb 6s character was confirmed based on the strong asymmetry of a Pb 4 f core-level spectrum and MND-model calculations. Our approach using core-level photoemission can be applied to investigate the conduction state of other compound materials, where valence-band photoemission is difficult to apply. Moreover, the failure of the DŠ lineshape indicates that, in general, we should use the more realistic DOS to explain the core-level lineshape of materials.

Methods

We synthesized $Ag_5Pb_2O_6$ single crystals using a previously reported self-flux method³¹. First, we mixed 6N- $AgNO_3$ (Sigma-Aldrich) and 5N- $Pb(NO_3)_2$ (Sigma-Aldrich) powders thoroughly and placed the mixture into an alumina crucible. We initially heated the mixture in air to 90° C and maintained that temperature for 3 hours. Then, we heated it at 405° C for 4 days. We varied the ratio between $AgNO_3$ and $Pb(NO_3)_2$ to obtain large crystals with a hexagonal stick shape. The size of the largest crystal is about $0.2 \times 0.2 \times 2$ mm³. We used the X-ray diffraction technique to confirm the crystal structure of the synthesized crystal. The diffraction pattern indicated that there was no secondary phase. We also confirmed the stoichiometry between Ag and Pb ions via the energy dispersive X-ray spectroscopy.

We performed core-level photoemission experiments at the Beamline 4A1 of Pohang Light Source. The single crystal was cleaved and measured at 50 K under a vacuum of 3×10^{-11} Torr. Possible cleavage planes are the Ag(1) and Ag(2) terminations as displayed in Fig. 1(a). To achieve the best energy resolution, we used photon energies of 480 eV for the Ag 3 $d_{5/2}$ level and 280 eV for the Pb 4 $f_{7/2}$ level. We determined the binding energy with reference to the 4 $f_{7/2}$ core-level peak of polycrystalline gold electrically connected to the sample. All measured spectra were reproducible for three samples.

References

1. Bednorz, J. G. & Müller, K. A. Possible high T_c superconductivity in the Ba-La-Cu-O system. *Zeitschrift für Physik B Condensed Matter* **64**, 189–193 (1986).
2. Basov, D. N. & Timusk, T. Electrodynamics of high- T_c superconductors. *Review of Modern Physics* **77**, 721–779 (2005).
3. Yonezawa, S. & Maeno, Y. Type-I superconductivity of the layered silver oxide $Ag_5Pb_2O_6$. *Physical Review B* **72**, 180504 (2005).
4. Oguchi, T. Electronic band structure and Fermi surface of $Ag_5Pb_2O_6$. *Physical Review B* **72**, 245105 (2005).
5. Sutherland, M., Mann, P. D. A., Bergemann, C., Yonezawa, S. & Maeno, Y. Nearly free electrons in the layered oxide superconductor $Ag_5Pb_2O_6$. *Physical Review Letters* **96**, 097008 (2006).
6. Tuoriniemi, J. *et al.* Superconductivity in lithium below 0.4 millikelvin at ambient pressure. *Nature* **447**, 187–189 (2007).
7. Brennan, T. D. & Burdett, J. K. Electronic structure of $Ag_5Pb_2O_6$. *Inorganic Chemistry* **33**, 4794–4799 (1994).
8. Bystrom, A. & Evers, L. The crystal structures of Ag_2PbO_2 and $Ag_5Pb_2O_6$. *Acta Chemica Scandinavica* **4**, 613–627 (1950).
9. Dickens, B. The bondings in Ag_2PbO_2 and $Ag_5Pb_2O_6$. *Journal of Inorganic and Nuclear Chemistry* **28**, 2793–2799 (1966).
10. Yoshii, K. *et al.* Neutron diffraction and X-ray absorption study of $Ag_5Pb_2O_6$. *Journal of Inorganic and Nuclear Chemistry* **180**, 377–381 (2007).
11. Yeh, J. J. & Lindau, I. Atomic subshell photoionization cross sections and asymmetry parameters: $1 \leq Z \leq 103$. *Atomic Data and Nuclear Data Tables* **32**, 1–155 (1985).
12. Im, H. J. *et al.* Direct observation of dispersive kondo resonance peaks in a heavy-fermion system. *Physical Review Letters* **100**, 176402 (2008).
13. Mahan, G. D. Excitons in degenerate semiconductors. *Physical Review* **153**, 882–889 (1967).
14. Nozières, P. & DeDominicis, C. T. Singularities in the X-ray absorption and emission of metals. III. one-body theory exact solution. *Physical Review* **178**, 1097–1107 (1969).
15. Ohtaka, K. & Tanabe, Y. Theory of the soft-X-ray edge problem in simple metals: historical survey and recent developments. *Review of Modern Physics* **62**, 929–991 (1990).
16. Doniach, S. & Šunjić, M. Many-electron singularity in X-ray photoemission and X-ray line spectra from metals. *Journal of Physics C: Solid State Physics* **3**, 285–291 (1969).
17. Shirley, D. A. High-resolution X-ray photoemission spectrum of the valence bands of gold. *Physical Review* **5**, 4709–4714 (1972).
18. Citrin, P. H., Wertheim, G. K. & Baer, Y. Surface-atom X-ray photoemission from clean metals: Cu, Ag, and Au. *Physical Review B* **27**, 3160–3175 (1983).
19. Hüfner, S. *Photoelectron Spectroscopy* (Springer-Verlag Berlin Heidelberg, 2003).
20. Tanuma, S., Powell, C. J. & Penn, D. R. Calculations of electron inelastic mean free paths. V. data for 14 organic compounds over the 50–2000 eV range. *Surface and Interface Analysis* **21**, 165–176 (1994).
21. Hüfner, S. & Wertheim, G. K. Core-line asymmetries in the X-ray-photoemission spectra of metals. *Physical Review B* **11**, 678–683 (1975).
22. Citrin, P. H., Wertheim, G. K. & Baer, Y. Many-electron effects in core-level X-ray and electron spectroscopies from Na, Mg, and Al. *Physical Review Letters* **35**, 885–888 (1975).
23. Baer, Y., Citrin, P. H. & Wertheim, G. K. X-ray photoemission from lithium: An explanation of its X-ray edge. *Physical Review Letters* **37**, 49–52 (1975).
24. Nyholm, R., Berndtsson, A. & Mårtensson, N. Core level binding energies for the elements Hf to Bi ($Z = 72–83$). *Journal of Physics C: Solid State Physics* **13**, 1091–1096 (1980).
25. Davis, L. C. & Feldkamp, L. A. Effect of electron correlations on photoemission from narrow-band metals. *Journal of Applied Physics* **50**, 1944–1949 (1979).
26. Davis, L. C. Photoemission from transition metals and their compounds. *Journal of Applied Physics* **59**, 25–63 (1985).
27. Wertheim, G. K. & Walker, L. R. Many-body effects in transition metals: role of the density of states. *Journal of Physics F: Metal Physics* **6**, 2297–2306 (1976).
28. Cowan, R. D. *The Theory of Atomic Structure and Spectra* (University of California Press, 1981).
29. Slater, J. C. The theory of complex spectra. *Physical Review* **34**, 1293–1322 (1929).
30. Fetter, A. L. & Walecka, J. D. *Quantum Theory of Many-Particle Systems* (McGraw-Hill Book Company, 2003).
31. Yonezawa, S. & Maeno, Y. Nonlinear temperature dependence of resistivity in single crystal $Ag_5Pb_2O_6$. *Physical Review B* **70**, 184523 (2004).

Acknowledgements

We thank T. Oguchi for providing the electronic-structure data of $\text{Ag}_5\text{Pb}_2\text{O}_6$. We also acknowledge the experimental support provided by H.K. Yoo and C.-T.Kuo. This work was supported by the Institute for Basic Science (IBS) in Korea (Grant No. IBS-R009-D1, IBS-R009-G2), and grants from the National Research Foundation of Korea (NRF) (2012M2B2A4029470, 2017R1C1B2004927). Experiments at PLS-II were supported in part by MSIP and POSTECH.

Author Contributions

S.S. and H.-D.K. conceived and designed the work. K.D.L., C.J.W., and N.J.H. synthesized $\text{Ag}_5\text{Pb}_2\text{O}_6$ single crystals. S.S., J.S.O., H.-D.K., and B.-G.P. carried out the core-level photoemission experiments. Fitting and analyses were conducted by S.S. and H.-D.K. The research was carried out with guidance from M.H., Y.J.C., C.K., H.-D.K., and T.W.N. S.S., H.-D.K., and T.W.N. co-wrote the manuscript. All authors discussed the work and reviewed the manuscript.

Additional Information

Competing Interests: The authors declare that they have no competing interests.

Publisher's note: Springer Nature remains neutral with regard to jurisdictional claims in published maps and institutional affiliations.



Open Access This article is licensed under a Creative Commons Attribution 4.0 International License, which permits use, sharing, adaptation, distribution and reproduction in any medium or format, as long as you give appropriate credit to the original author(s) and the source, provide a link to the Creative Commons license, and indicate if changes were made. The images or other third party material in this article are included in the article's Creative Commons license, unless indicated otherwise in a credit line to the material. If material is not included in the article's Creative Commons license and your intended use is not permitted by statutory regulation or exceeds the permitted use, you will need to obtain permission directly from the copyright holder. To view a copy of this license, visit <http://creativecommons.org/licenses/by/4.0/>.

© The Author(s) 2017